Proceedings of the ASME 2023
International Design Engineering Technical Conferences & Computers and Information in Engineering Conference
IDETC2023
August 20–August 23, 2023, Boston, MA

IDETC2023-116542

A FRAMEWORK FOR ORIGAMI FLASHER PATTERN OPTIMIZATION TO MITIGATE RIGID-FOLDABILITY ISSUES

Nathan Coleman[1,†], Katie Varela[1,†,*], Mitchel Skinner[1], Larry L. Howell[1], Spencer P. Magleby[1]

[1]Brigham Young University, Provo, UT

ABSTRACT

Origami is increasingly popular in engineering for its ability to deploy to a large area from a compact volume. In addition to its circular nature and fixed central polygon, the origami Flasher pattern has several advantages that make it a desirable candidate for many deployable systems, including space applications such as LiDAR telescopes, solar arrays, or reflectarray antennas. Some complications with the Flasher pattern that limit its application are panel interference due to multiple high degree vertices and its inability to rigidly fold. This work builds on the Cross-Frame design by Varela et al., which was implemented as a thickness accommodation technique, as well as a solution for the interference issues. Modifications of the Cross-Frame design for the Flasher origami pattern are presented, which address interference and the rigid-foldability issues within the Flasher pattern. Three frame designs, the modified cross, the diamond, and the Z design, are presented and trade-offs for each design regarding stiffness, either localized or generalized, are explored. Methods for optimizing each frame design to accommodate for rigid-foldability are introduced and algorithms and constraints for this topological optimization are discussed. Results of optimizations for stiffness and length are shown, and further modifications for future research are discussed.

Keywords: Origami, Flasher pattern, Optimization, Rigid-foldable

NOMENCLATURE

Analytical Model

k	Rotational beam stiffness [Nm/rad]
L	Beam length [m]
E	Modulus of elasticity [Pa]
I	Moment of inertia [kgm^2]
q	Distance from edge of beam to point moment [m]
θ	Angle between the beam element and the point moment vector [rad]

Optimization Model

χ	Ratio of stiffnesses along bisection and non-bisection lines, respectively
e	Associated with edge points being optimized for each panel
m	Associated with middle points being optimized for each panel
c	Associated with corner points for each panel
$line_n$	Associated with edge lines for each panel
G	Associated with opposite edge of a gore
τ	Minimum distance from an path end point to a panel vertex
$\mathscr{L}$	Total length of beam segments

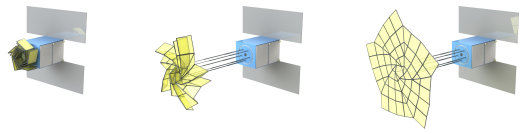

FIGURE 1: EXAMPLE FLASHER CONFIGURATION. A) STOWED. B) MID-DEPLOYMENT. C) DEPLOYED.

1. INTRODUCTION

Folded mechanical systems based on origami patterns have the ability to change their shape during their folding or unfolding process. This ability has often been used to compactly stow large arrays [1], though origami-based designs have recently been used for many additional engineering applications [1–3]. Principles of origami have been used to inspire deployable structures used in aerospace design, including a self-stiffening and retractable deployable space array [4], a foldable antenna [5–8], and a deployable Flasher-patterned solar array [9, 10]. This work will address space-related applications of origami, but the principles here are not limited to those usages.

[†]Joint first authors
[*]Corresponding author: katievarela@byu.net

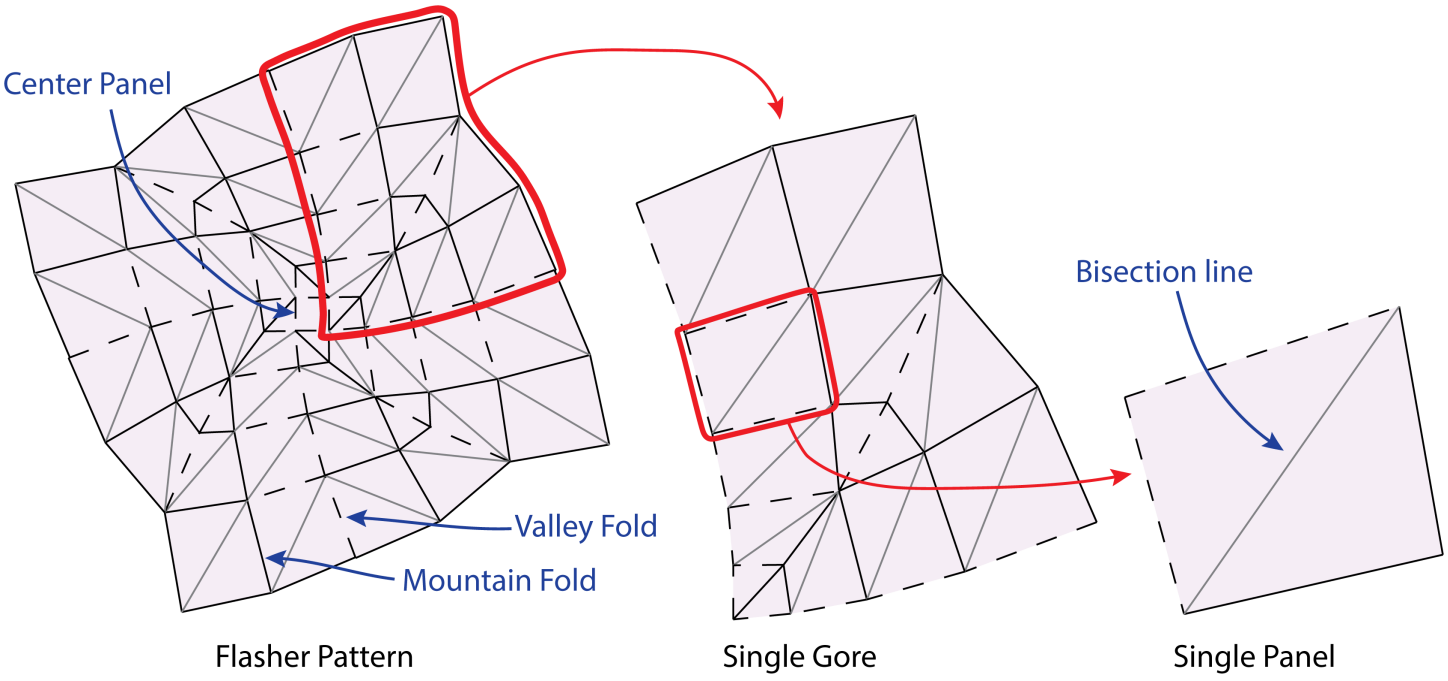

FIGURE 2: THE FLASHER CONFIGURATION SELECTED FOR THE OPTIMIZATION WITH PARAMETERS $m = 4$, $r = 2$, $h = 2$, $dr = 0.2$. NOTE THAT MOUNTAIN FOLDS ARE SHOWN AS SOLID LINES AND VALLEY FOLDS ARE SHOWN AS DASHED LINES. BISECTION LINES ARE SHOWN IN LIGHT GRAY.

Many space applications, such as solar arrays, reflectarray antennas, and LiDAR telescopes, require large, flat surface areas. Therefore, these arrays need to be able to easily transform from a compact volume into a relatively large deployed area. Because origami patterns tend to be compact when stowed, they can be well suited for space applications.

An origami pattern that has been of interest for space and other applications is called the Flasher [10–13]. An example of Flasher deployment is shown in Fig. 1. This pattern's key benefit is its ability to be compact when stowed, then open to have an array with a large area-to-volume ratio. Other benefits of the Flasher include that it is generally circular in nature, extensible by adding more rings, and has a central panel that can be used for anchoring. The Flasher is not a flat-folding pattern, but instead wraps around itself as it is stowed, achieving a flat state only when fully deployed. The Flasher is also not rigid-foldable.

Tachi describes rigid-foldable origami (or rigid origami) as "piecewise linear origami that is continuously transformable without the deformation of each facet" [14]. In other words, if a panel is not rigid-foldable, the panel itself must deform or bend during the transition between stowed and deployed, instead of having all of the motion in the folds [14–16].

The Flasher pattern was adapted to create a solar array, using a membrane hinge approach that reduced the rigid-foldability complications [9, 13]. Additional work has been done to accommodate thickness in the Flasher for other space-related applications [17, 18], because using materials with any finite thickness affects the pattern's ability to fold [19].

This work modifies structural topology of Flasher panels to help address the complications due to rigid-foldability. The model was proposed by Varela et al. [18], called the Cross-Frame, and is used for both thickness accommodation and structural support for the Flasher array. That initial work puts the frames through the center of the panels, preventing interference issues by keeping material away from the vertices. This paper considers topological features to reduce issues with rigid-foldability by modifying the geometry (similarly implementing the principle that link shape does not matter for kinematic motion), but does not address thickness accommodation directly.

Our objective in this work is to create a framework to optimize the structural support for the Flasher panels so that they can deflect as needed, while maintaining the stiffness of the array in the deployed state. In other words, to create a localized region of stiffness in the panel, so the panel can be flexible in one direction, but stiff overall. In this work, the compliance of the panel geometry achieves a slight deflection along the bisection line (shown in Fig. 2), which allows the pattern to fold with semi-rigidity, while maintaining the original number of panels, fold lines, and degrees of freedom as the origami pattern.

2. BACKGROUND

The Flasher has four parameters that describe its configuration: m, r, h, and dr, which are described in detail by Zirbel et al. [9]. For this optimization, the Flasher selected has parameter values of $m = 4$, $r = 2$, $h = 2$, and $dr = 0.2$, as shown in Fig. 2. These parameters where chosen because they represent a Flasher with a typical deployed area to stowed volume ratio. Because $m = 4$, the Flasher has four repeating sections, called gores, that have rotational symmetry.

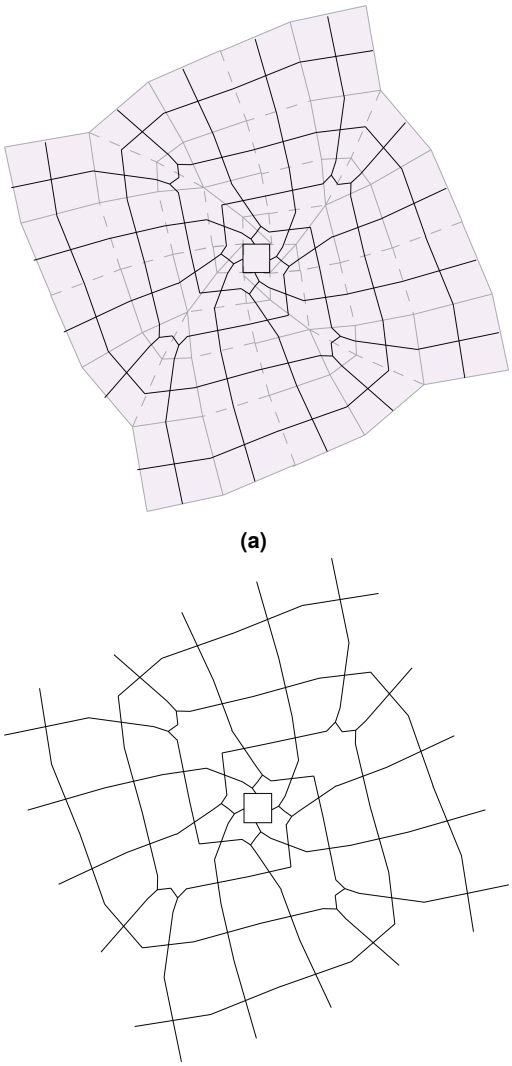

FIGURE 3: EXAMPLE CROSS-FRAME FLASHER CONFIGURATION. A) WITH PANELS FOR REFERENCE. NOTE THAT THE CROSS-FRAME INTERSECTS EACH FRAME EDGE LINE AT ITS MIDPOINT. B) WITH NO PANELS.

2.1 Rigid-Foldability

Because the Flasher is not rigid-foldable, it is multi-stable. Whether folding in paper or in thickened materials, there is an unstable equilibrium point that the Flasher goes through in the process of stowed-to-deployed (or vice versa). This creates a "snap", or a high potential energy intermediate state that must be overcome during the deployment process.

Previous work to accommodate for this issue involves bisecting all of the four-sided panels into triangles [20], which makes the Flasher rigid-foldable and avoids the snap issue, but increases the complexity of the pattern by significantly increasing the total number of panels and required hinges.

Another method proposed uses kirigami, which is similar to origami, but involves cutting the material instead of folding it [8]. Transitioning an origami pattern to a kirigami pattern can introduce additional degrees of freedom which can lead to challenges in system deployment and panel alignment.

To avoid these complications, this work has developed a program to optimize the shape of each Flasher panel's structure to reduce the stiffness along the bisection line outlined by Lang in [20] making it compliant along the bisection direction, while maximizing stiffness in the pattern in other directions.

2.2 Compliant Mechanisms

Origami-based design has become a branch of compliant mechanism research, inspiring an alternative solution to traditional design methods by using flexible members to replace traditional hinges, joints, and other moving parts [3]. Compliant mechanisms are often modeled as pseudo-rigid bodies that have torsion springs with variable stiffness, k, depending on their material, geometry, and end conditions. The support structures proposed for the Flasher have stiffness that is inversely proportional to the length of the beams.

By modeling these support segments as simply supported beams, they can be treated as springs in parallel. Therefore, the equivalent stiffness of the panel diagonals is the sum of the individual stiffnesses that touch the respective diagonals. According to this assumption, to minimize stiffness along the bisection line it is ideal to have fewer beams in that direction, and more beams in the directions that are intended to be stiff.

3. METHODS

3.1 Overview

The design approach behind the Cross-Frame Flasher seeks to take a panel made up of a regular polygon with three or four sides and shift the structure away from the vertices to avoid complications during thickness accommodation and folding. Figure 3 shows this approach applied to a full Flasher pattern and Fig. 4 shows a single panel from that Flasher pattern. Because these panels need to be able to connect to each other, it is necessary to have at least one hinge along each panel edge. The work done in [18] applied this methodology to an entire Flasher by placing the Cross-Frame at the center of each panel polygon, or in other words, having the hinge locations at the midpoints of each edge, shown in Fig. 4.

This work sought to build on the original Cross-Frame by optimizing the placement of the elements within each panel using three different methods, called "the optimized cross", "the diamond", and "the Z frame", shown in Figs. 5, 6, and 7, respectively. These three designs were derived from the condition that each panel must connect to each adjacent panel by at least one point, and as such all contain one point along each panel edge, although they differ in how they connect the edge points.

The model used here initially sought to minimize the total length of the frame, which was used as a surrogate for maximizing the overall stiffness due to the inverse relationship between length and stiffness. From this criterion, the optimized cross design was created by selecting points for the hinge locations and the middle point that would minimize each beam's length. Because of this modification, a major difference between this design and the original Cross-Frame design is that cross elements are not constrained to be at the midpoint of the panel edges. An example of the modified cross design is shown in Fig. 5.

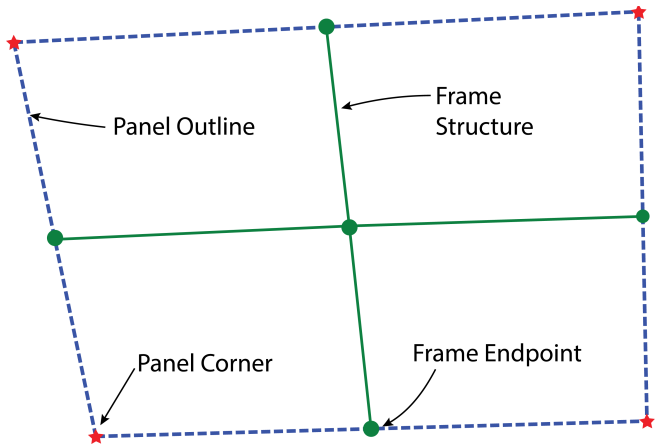

FIGURE 4: ILLUSTRATION OF INITIAL CROSS-FRAME DESIGN. NOTE THAT FRAME STRUCTURE IS SHOWN IN GREEN, PANEL OUTLINES ARE SHOWN IN BLUE, AND PANEL CORNERS ARE SHOWN IN RED. THE DOTS AROUND THE EDGE INDICATE HINGE PLACEMENT.

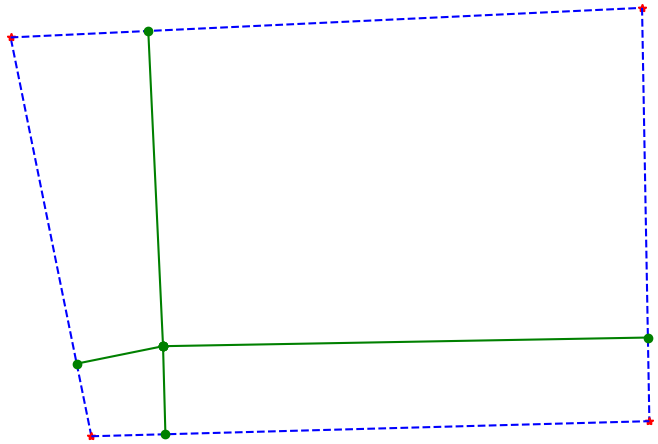

FIGURE 5: MODIFIED CROSS DESIGN, SHOWN OPTIMIZED TO MINIMIZE LENGTH.

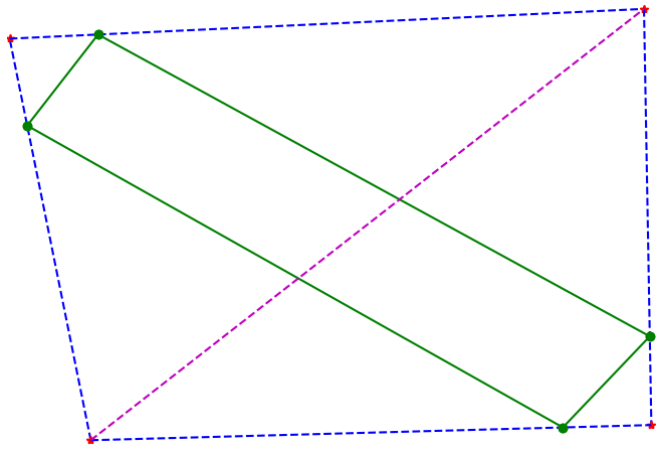

FIGURE 6: DIAMOND FRAME DESIGN, SHOWN OPTIMIZED FOR STIFFNESS. BISECTION LINE IS SHOWN IN DASHED MAGENTA.

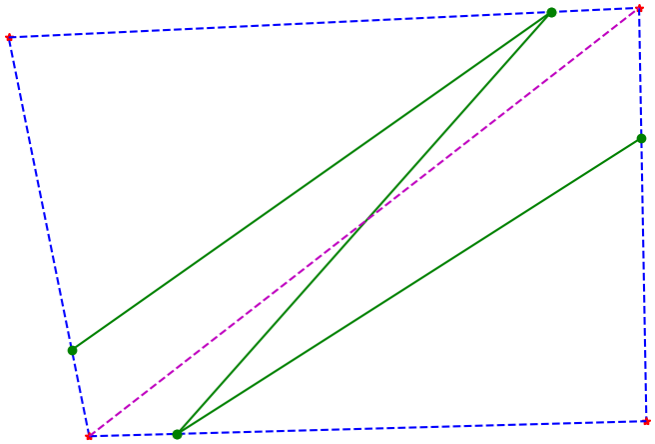

FIGURE 7: Z-FRAME DESIGN, SHOWN OPTIMIZED FOR STIFFNESS. BISECTION LINE IS SHOWN IN DASHED MAGENTA.

However, because the Flasher design requires bisections on quadrilateral panels in order to be rigid-foldable, our objective was not to maximize the stiffness of every panel, but rather to minimize the stiffness of the frame along the bisection axis and stiffen it in the axis opposite to the bisection. These diagonals are predefined by the pattern, or the panel boundaries themselves, and do not change with the shape of the support structure. This constraint led to the development of two different designs which include no middle point and connect the edge points directly to each other.

The first is referred to as the "diamond frame" design, in which the frame makes a diamond shape in connecting to all edge points, shown in Fig. 6. This design was derived from basic compliant mechanism principles - long members flex more than short members (with the same material, cross-section, applied force/moment, etc.) [3], and therefore, it uses short beams in the directions that require stiffness and longer beams in the directions that require flexibility. The diamond design has an analytical advantage of maintaining an overall stiffness for each panel while allowing for reduced stiffness along one axis.

The second design without a central connection point is referred to as the "Z frame" design (see Fig. 7), which functions according to the same principle as the diamond, but uses only three members to connect all four sides. The theory behind this design is that it minimizes the frame structure required to connect each panel, though this could make it less stiff overall. It can be noted that there are four possible Z orientations to connect the edge points of each panel, and the orientation chosen reflects the minimization of stiffness in the desired direction to aid in folding.

Each of these three panel frame designs were used and compared in the optimization of the full Flasher to compare the advantages and disadvantages of each. Once the optimization of each panel was set up, adjacent panels could be optimized together by having the panels share common edge points. This approach was used to optimize an entire gore of the Flasher for each frame design described, as shown in Figs. 9, 10, and 11. The optimization of a single gore of the Flasher was able to be used as a surrogate for the entire Flasher by adding an additional constraint to keep points on the edge of the gore aligned with their corresponding points on the opposite edge.

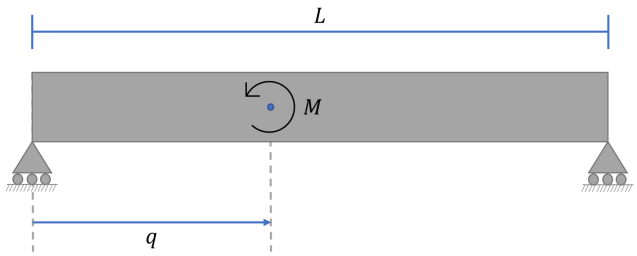

FIGURE 8: MODEL USED FOR EACH OF THE BEAMS WITHIN THE OPTIMIZED DESIGNS.

Once the optimization was found to be working correctly for each method with a full Flasher, various stiffness models were analyzed for their potential implementation, and a relative stiffness model was chosen. To accomplish the goal of achieving stiffness in all directions except along the bisection line, the optimization was able to vary the x and y positions of all points along the sides of each panel, subject to the polygon boundaries, the panel edge lines, minimum distance constraints between points, and symmetry between gore edges.

3.2 Analytical Stiffness Model

Calculating the stiffness of these structures is complicated by the variety of configurations that can be utilized, and the boundary conditions depend somewhat on the selected configuration. For this work, a simply supported beam with a point moment on the beam span was selected as the basic model, as shown in Fig. 8.

It was assumed that the magnitude of the moment caused by the panel bending would be equivalent on each beam, and that the vector component that is parallel to the beam (causing torsion) is negligible compared to the bending component. With these assumptions and a fixed cross-section and material, the stiffness equation $k = M/\theta$ is the general form for stiffness with bending moments, so the equations for M and θ associated with a simply supported beam with a point moment at an arbitrary distance were substituted in, which simplifies to

$$k_q = \frac{3EIL\sin\theta}{L^2 - 3Lq + 3q^2} \tag{1}$$

where the bending moment component, $\sin\theta$, is determined by the angle that is made between the beam element and the moment vector. The variable q is defined as

$$q = RL \tag{2}$$

where R is a fraction that describes how far along the beam the moment is acting, and $R\epsilon[0,1]$. Because of the symmetry, it does not matter whether q is measured from the "left" or the "right" end of the beam, so RL can be substituted for q, allowing the Eq. (1) to simplify further, canceling out the L in the numerator by factoring an L from each term in the denominator. This factor also weights the equations to get a maximum stiffness by applying the moment at the center of the beam, and a minimum by applying the moment at the edges.

A ratio of the stiffnesses was calculated along the bisection line versus along the "non-bisection" line, as shown in Eq. (3)

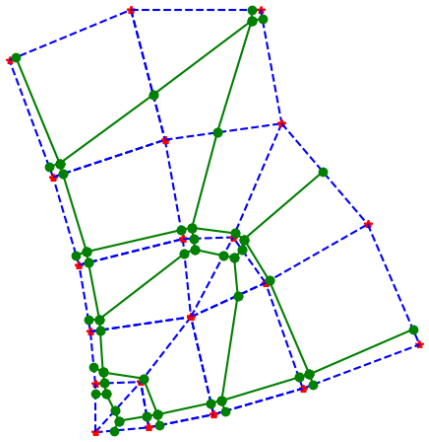

FIGURE 9: CROSS DESIGN OPTIMIZED TO MINIMIZE TOTAL LENGTH OF FRAME ELEMENTS WHILE VARYING LOCATIONS OF POINTS ALONG EACH PANEL EDGE AND PANEL MIDDLE.

below. By using a ratio of stiffness, the assumptions of the beam end conditions, as well as values for modulus of elasticity and moment of inertia of the beam, will be present in both the numerator and the denominator and therefore cancel out and not affect the calculated result. The resulting stiffness ratio, χ, is

$$\chi = \frac{k_{Bisection}}{k_{Non-Bisection}} = \frac{L_{NB}(1 + 3R_{NB} + 3R_{NB}^2)\sin\theta_B}{L_B(1 + 3R_B + 3R_B^2)\sin\theta_{NB}} \tag{3}$$

Eq. (3) will be used as the objective function, which will minimize the stiffness along the bisection line and maximize the stiffness along the other diagonal by varying L, R, and θ for both diagonals.

Because the modified cross method yielded segments that do not intersect with either the bisection or non-bisection lines, the stiffness calculation ratio described above is not effective. Therefore, the cross structure shown in Fig. 9 only minimizes length, and does not have stiffness ratios associated with it. Additionally, for all three designs, the triangular panels in each gore do not have bisection lines, so they also were calculated to minimize length, since they do not need to flex during deployment, and therefore can have maximum stiffness.

3.3 Optimization Details

The problem formulation used to optimize the frame of a single panel and a full Flasher gore is given in Table 1, which minimizes the objective function given in Eq. (3), subject to constraints 1-6. This same method was used for optimizing the entire Flasher, with the addition of constraint 7, which keeps adjacent Flasher gores aligned. Note that constraints 1 and 7 are equality constraints, while constraints 2 through 6 are inequality constraints.

To optimize the pattern, initial guesses were selected for each point using the midpoint of the corresponding panel edge. Additionally, for the optimized cross, the initial guess for the center point was determined from the middle of the panel. It should be noted that single-panel optimizations using the listed constraints presented several equivalent local minima when optimizing for

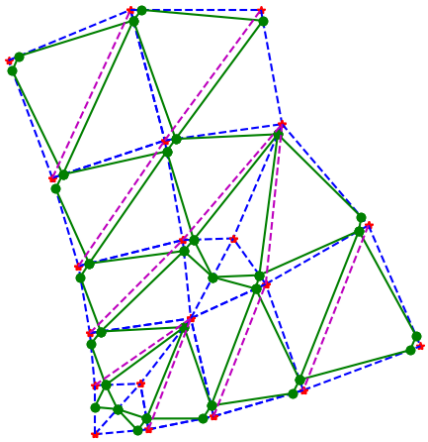

FIGURE 10: DIAMOND DESIGN OPTIMIZED TO MINIMIZE THE RATIO OF STIFFNESS ACROSS THE BISECTION LINE TO THE STIFFNESS ACROSS THE NON-BISECTION LINE, WHILE VARYING LOCATIONS OF POINTS ALONG EACH PANEL EDGE. NOTE THAT THIS IS DONE BY MINIMIZING THE STIFFNESS ACROSS THE BISECTION LINE AND MAXIMIZING THE STIFFNESS ACROSS THE NON-BISECTION LINE.

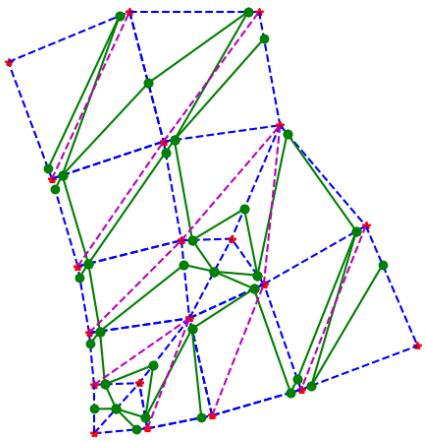

FIGURE 11: Z DESIGN OPTIMIZED TO MINIMIZE THE RATIO OF STIFFNESS ACROSS THE BISECTION LINE TO THE STIFFNESS ACROSS THE NON-BISECTION LINE, WHILE VARYING LOCATIONS OF POINTS ALONG EACH PANEL EDGE. NOTE THAT THIS IS DONE BY MINIMIZING THE STIFFNESS ACROSS THE BISECTION LINE AND MAXIMIZING THE STIFFNESS ACROSS THE NON-BISECTION LINE.

length, and as such, it should be acknowledged that the optimization of full Flasher gore represents one of several potential configurations. To account for this, additional constraints should be added for thickness accommodation, manufacturing, and general feasibility as needed. Because each gore is identical, the optimization is determined for panels on one gore, with considerations (via constraints) of how each gore would connect to the next. Note that the gores are staggered as they wrap around the central polygon, which the optimization also takes into account.

Constraint 1 is used to keep each optimal edge point on its associated panel edge line. Constraint 2 is used to keep each optimal middle point (when using the modified cross pattern) within the bounds of its associated panel.

Constraints 3 through 6 use Euclidean distance to avoid trivial solutions where multiple points are at the same location or points are at panel vertices. These are necessary to maintain the benefit of the Cross-Frame design by creating space between the frame and the panel vertices to avoid interference issues at each vertex. The parameter "τ" is used to define the minimum allowable distance between points. Constraint 3 compares each hinge location to every other hinge location, to make sure they do not find the same optimal position. Although this constraint recommends that every hinge point be checked for the minimum distance, the speed of the optimization can be significantly improved by checking only the "nearest neighbors" or adjacent points. Note that constraint 3 does not check each edge point against itself. Constraint 4 is applicable only for the modified cross design, and determines if the distance between the middle point and the edge points is smaller than τ. Constraints 5 and 6 check if the edge points and middle points (again, only for the modified cross approach) are far enough away from the corners of their panel, respectively.

Constraint 7 also uses Euclidean distance (or 2-norm) to extrapolate the optimization of a single gore out to the entire Flasher by constraining the optimal points on the edges of the each gore to be at equal distances from their associated corners; in other words, this algorithm ensures that the connection points from gore to gore will align with each other in order to create a continuous frame.

The optimization algorithm used in this work was the python SciPy "minimize" package, and the supplementary algorithms that were created for the constraints are not included in this work for conciseness.

TABLE 1: OPTIMIZATION PROBLEM FORMULATION

$$
\begin{aligned}
\text{minimize} \quad & \chi \\
\text{by varying} \quad & (x,y)_e \\
\text{subject to} \quad & (x,y)_e \in line_n && (1)\\
& (x,y)_m \in (x,y)_c && (2)\\
& \|(x,y)_{e_i} - (x,y)_{e_j}\|_2 \geq \tau, \; for \; i \neq j && (3)\\
& \|(x,y)_e - (x,y)_m\|_2 \geq \tau && (4)\\
& \|(x,y)_e - (x,y)_c\|_2 \geq \tau && (5)\\
& \|(x,y)_m - (x,y)_c\|_2 \geq \tau && (6)\\
& \|(x,y)_e - (x,y)_c\|_2 = \\
& \quad \|[(x,y)_e^G - (x,y)_c^G\|_2 && (7)
\end{aligned}
$$

4. RESULTS

For the diamond and the Z methods, the optimizer was effectively able to vary L, R, and θ for each of the diagonals, maximizing L_B, R_B, and $\sin\theta_{NB}$ and minimizing L_{NB}, R_{NB}, and $\sin\theta_B$, as shown in Eq. (3). Observations of the resulting optimizations demonstrated that the R values and the $\sin\theta$ values were driving factors, particularly in the diamond method (see Fig. 10).

Because of the trade-offs with length, angles, number of beams, etc. described above, the proposed optimization output

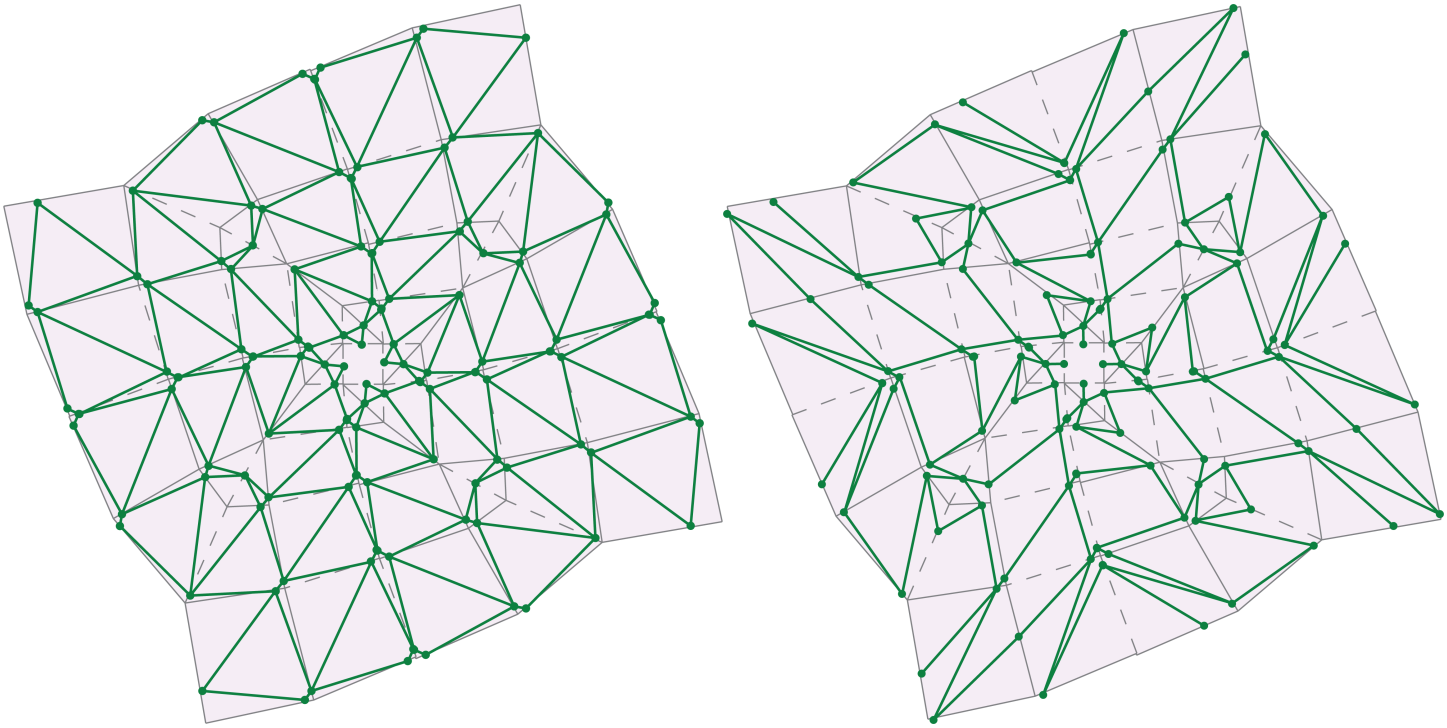

(a) Diamond design. (b) Z design.

FIGURE 12: FULL FLASHER OPTIMIZATION SHOWN OVERLAID WITH ORIGINAL PATTERN.

therefore is analytically feasible. In other words, there is evidence that this framework is a valid method for implementing compliance into rigid-foldable origami patterns.

The resulting optimized gores for each frame design can be seen in Figs. 9-11. Note that the bisection lines are shown in red for Figs. 10 and 11, but not for Fig. 9, because the modified cross design was not optimized around stiffness.

5. DISCUSSION

5.1 Modified Cross Design

Length minimization was used for the modified cross design. The results in Fig. 9 brought the cross intersection point as close to a vertex as possible (considering the constraints), and often had most of the hinge points surrounding a vertex. For this design, the results were mostly intuitive, though because all the panels needed to connect with each other, there are some angles that were less obvious. Still, this optimization was able to maintain the space around the vertices, especially around the degree-six vertex that has the most interference. This method was not modified for bisection line flexibility, so no conclusions will be drawn regarding that objective.

The modified cross design, because it does not have an accurate stiffness ratio, is not recommended for addressing the issue with rigid-foldability. However, a different stiffness calculation method could be utilized to achieve this objective.

5.2 Diamond Design

Although the single panel optimization yielded a topology of a rectangular structure, optimizing the full gore of panels led to much more trapezoidal results for each panel. This optimized solution with the diamond method was not anticipated, but it seems effective, because the optimizer emphasized the R and $\sin\theta$ terms, instead of focusing on the L terms from Eq. (3). The beams that intersect with the bisection lines therefore aren't perpendicular with the bisection line, and their intersection points are close to the ends of the beam, while the beams that intersect the non-bisection line are almost perfectly perpendicular, and intersect near the midpoint of each beam. Even though one of the beams adding to k_{NB} is long (which is typically more flexible), the optimization determined that it didn't contribute as much as the angle and R value.

The results of this optimization also remained close to the vertices, but instead of surrounding the vertices on three sides like the modified cross method did, it only drew in two of the hinge points close to the vertices, as shown in Fig. 10. The degree six vertex does have one hinge point close by, but interference would still be minimal due to constraints 3-6. The diamond method's solution is also nearly symmetrical, which implies a more stable structure overall.

The stiffness ratios per panel for this method were approximately 10:1, non-bisection to bisection, according to the optimization. Although the results have not been prototyped and confirmed yet, this technique is a good candidate for achieving a structure that will accommodate the rigid-foldability issue while maintaining reasonable stiffness when deployed.

5.3 Z Design

The solution found by the optimizer for a single panel of the Z design was as expected: the bisection line was only intersected by one of the support beams, while all three beams intersected

the non-bisection line, increasing the stiffness in that direction. Additionally, the beam that touches the bisection line is nearly parallel to it, minimizing the intersection angle, and the others are nearly all perpendicular to the other diagonal (see Fig. 11). The L values seem less significant to the optimization than the angle and the intersection ratio.

The hinge points clustering around the vertices were not as predictable in this design, as some vertices have only one hinge point nearby, and others have three. The results were also not symmetric, which was unanticipated, and in particular, the geometry close to the degree-six vertex is not intuitive.

The middle segment of the Z is treated similar to a torsion bar, which helps with flexing, though because it did not take torsion into consideration, it would likely have an even higher stiffness ratio (i.e.able to flex even more along the bisection line). With that considered, the Z design without taking torsion into account had an average ratio of about to 20:1. This design, therefore, is also a good candidate for the structure, depending on the flexibility needed within the panels.

5.4 Summary and Future Work

Using the simply supported beam model, this work was able to develop designs for the frame of a Flasher origami pattern that helps address rigid-foldablity complications, allowing for a variety of panel flexibility needs. Fig. 12 shows a representation of how a fully optimized Flasher pattern would look for each design, with an optimized gore rotationally mirrored about the central polygon, though further experimentation and prototyping could validate whether this satisfies the rigid-foldability condition for the full Flasher.

Future work could benefit from using a "mix and match" approach to the optimization of the Flasher by allowing the optimizer to choose which frame design is used on a panel-by-panel basis, rather than using the same frame design for every panel. In this way the optimization could accommodate the different requirements for each Flasher panel; for example, panels on the outer edge are larger, and would therefore require more compliance along their bisection lines to fold, as well as requiring more stiffness along the non-bisection lines to support the Flasher structure when deployed.

Additional future work recommended would be to validate the full Flasher optimization results using finite element analysis such as ANSYS, or other beam models. Prototyping of these designs is in work at BYU, but has not yet been completed.

6. CONCLUSION

This optimization is meant as a framework to help resolve rigid-foldable complications with the Flasher pattern, and shows the feasibility of creating a Flasher structure that has flexible panels. This work demonstrates the feasibility of creating a Flasher that can withstand the rigid-foldability issues, using either the diamond or Z designs. This optimization framework may also be applicable to other rigid-foldable origami patterns.

ACKNOWLEDGMENTS

This work has been funded by the Air Force Research Lab/U.S. Space Force, through award number FA9453-22-C-0013, as well as the Transforming Antenna Center at Florida International University, and the Utah NASA Space Grant Consortium. Additional thanks to Dr. John Salmon, Dr. Brady Davies, Lais Oliveira, Hunter Pruett, Ivy Running, and Jake Sutton for their inputs on this project.

REFERENCES

[1] Filipov, Evgueni T, Tachi, Tomohiro and Paulino, Glaucio H. "Origami tubes assembled into stiff, yet reconfigurable structures and metamaterials." *Proceedings of the National Academy of Sciences* Vol. 112 No. 40 (2015): pp. 12321–12326.

[2] Kuribayashi, Kaori, Tsuchiya, Koichi, You, Zhong, Tomus, Dacian, Umemoto, Minoru, Ito, Takahiro and Sasaki, Masahiro. "Self-deployable origami stent grafts as a biomedical application of Ni-rich TiNi shape memory alloy foil." *Materials Science and Engineering: A* Vol. 419 No. 1 (2006): pp. 131–137.

[3] Howell, Larry L. *Compliant mechanisms*. John Wiley & Sons (2001).

[4] Pehrson, Nathan A, Ames, Daniel C, Smith, Samuel P, Magleby, Spencer P and Arya, Manan. "Self-deployable, self-stiffening, and retractable origami-based arrays for spacecraft." *AIAA Journal* (2020): pp. 1–8.

[5] Liu, Xueli, Georgakopoulos, Stavros V and Rao, Sudhakar. "A design of an origami reconfigurable QHA with a foldable reflector [antenna applications corner]." *IEEE Antennas and Propagation Magazine* Vol. 59 No. 4 (2017): pp. 78–105.

[6] Kaddour, Abdul-Sattar, Zekios, Constantinos L and Georgakapoulos, Stavros V. "A reconfigurable origami reflectarray." *2020 14th European Conference on Antennas and Propagation (EuCAP)*: pp. 1–4. 2020. IEEE.

[7] Russo, Nicholas E, Zekios, Constantinos L and Georgakopoulos, Stavros V. "A Capacity Reconfigurable Multimode Origami MIMO Antenna." *2019 IEEE International Symposium on Antennas and Propagation and USNC-URSI Radio Science Meeting*: pp. 411–412. 2019. IEEE.

[8] Lee, Sukwon, Shah, Syed Imran Hussain, Lee, Han Lim and Lim, Sungjoon. "Frequency-reconfigurable antenna inspired by origami flasher." *IEEE Antennas and Wireless Propagation Letters* Vol. 18 No. 8 (2019): pp. 1691–1695.

[9] Zirbel, Shannon A, Lang, Robert J, Thomson, Mark W, Sigel, Deborah A, Walkemeyer, Phillip E, Trease, Brian P, Magleby, Spencer P and Howell, Larry L. "Accommodating thickness in origami-based deployable arrays." *Journal of Mechanical Design* Vol. 135 No. 11.

[10] Guang, Chenhan and Yang, Yang. "An approach to designing deployable mechanisms based on rigid modified origami flashers." *Journal of Mechanical Design* Vol. 140 No. 8.

[11] Srinivas, Vivek and Harne, Ryan L. "Directing acoustic energy by flasher-based origami inspired arrays." *The Journal of the Acoustical Society of America* Vol. 148 No. 5 (2020): pp. 2935–2944.

[12] Lang, Robert J, Magleby, Spencer and Howell, Larry. "Single degree-of-freedom rigidly foldable cut origami flashers." *Journal of Mechanisms and Robotics* Vol. 8 No. 3 (2016): p. 031005.

[13] Zirbel, Shannon A. "Compliant Mechanisms for Deployable Space Systems." Ph.D. Thesis, Brigham Young University. 2014.

[14] Tachi, Tomohiro et al. "Rigid-foldable thick origami." *Origami* Vol. 5 No. 5 (2011): pp. 253–264.

[15] Watanabe, Naohiko and Kawaguchi, Ken-ichi. "The method for judging rigid foldability." *Origami* Vol. 4 (2009): pp. 165–174.

[16] Akitaya, Hugo, Demaine, Erik D, Horiyama, Takashi, Hull, Thomas C, Ku, Jason S and Tachi, Tomohiro. "Rigid foldability is NP-hard." *arXiv preprint arXiv:1812.01160* .

[17] Bolanos, Diana, Varela, Katie, Sargent, Brandon, Stephen, Mark A., Howell, Larry L. and Magleby, Spencer P. "Selecting and Optimizing Origami Flasher Pattern Configurations for Finite-Thickness Deployable Space Arrays." *Journal of Mechanical Design* Vol. 145 No. 2. DOI 10.1115/1.4055900. 023301.

[18] Varela, Katie, Oliveira, Lais, Sargent, Brandon, Howell, Larry L and Magleby, Spencer P. "Thickness Accommodation for the Flasher Origami Deployable Array." *AIAA SCITECH 2023 Forum*: p. 0944. 2023.

[19] Lang, Robert J, Tolman, Kyler A, Crampton, Erica B, Magleby, Spencer P and Howell, Larry L. "A review of thickness-accommodation techniques in origami-inspired engineering." *Applied Mechanics Reviews* Vol. 70 No. 1.

[20] Lang, RJ. "Tessellatica." (2021).